Bionanotechnology

DOI: 10.1002/anie.201206107

Observation of Multiphoton-Induced Fluorescence from Graphene Oxide Nanoparticles and Applications in In Vivo Functional Bioimaging**

*Jun Qian, Dan Wang, Fu-Hong Cai, Wang Xi, Li Peng, Zhen-Feng Zhu, Hao He, Ming-Lie Hu, and Sailing He**

Since it was first discovered,[1] graphene has consistently been a hot research topic owing to its unique electronic and mechanical properties.[2] Graphene also possesses special optical performance (saturable absorption, surface-enhanced Raman scattering), and has already shown wide application in for example mode-locking pulsed lasers, solar cells, and molecule sensing.[3] However, graphene has rarely been applied in bio-photonics research, which is mainly due to its non-dispersity in water. As a derivative of graphene, graphene oxide (GO) has many advantages.[4] GO is mainly comprised of carbon and it is non-toxic and more biocompatible[5] than other existing nanoparticles, such as heavy metal ions (quantum dots), noble metals (gold/silver nanoparticles), and rare-earth ions (upconversion nanocrystals).[6] GO is usually synthesized by partially oxidizing graphene, and the formation of graphitic islands on its surface is expected to produce a quantum confinement effect, which can open up a band gap in graphene as well as make GO possess photoluminescence performance.[7] Single-layered thin GO has every atom (two sides) exposed on its surface, giving it an extremely large surface area and leading to a higher drug/biomolecule loading efficiency (according to some theoretical analysis[4b] and experiment[8]) compared with CNTs and other nanoparticles. Second, GO also has a distinct photothermal effect, which is similar to some noble-metal nanoparticles. The use of GO has thus been increasingly investigated in recent years in in vitro bioimaging as a luminescent probe, in anticancer drug delivery as a molecule carrier, and in photodynamic therapy of tumors as a photon-thermal transducer.[9]

Although research on single photon (or downconversion) induced photoluminescence and two-photon absorption-only behaviors of GO have already been presented,[10] its multiphoton (or upconversion) induced photoluminescence performance has not been reported. Multiphoton excitation induced bioimaging has many unique advantages.[11] Owing to a square/cube or higher dependence of multiphoton absorption on laser intensity, the sample region outside the beam focus cannot be excited, and it could reduce the possibility of photobleaching of the sample signal.[12] The nonlinear excitation mode also helps to improve the spatial resolution of imaging, as only the site where the laser beam is focused can be efficiently excited. More importantly, multiphoton excitation has great potential for deep-range tissue imaging. For one-photon bioimaging, photosensitizers usually absorb light in the visible spectral region below 700 nm, where light penetration into the tissue is limited. On the other hand, two-photon excitation wavelength is usually in the range of 700–900 nm or 1000–1350 nm, and three-photon excitation wavelength is usually in the range of 1000–1350 nm. The 700–900 nm wavelength range is typically considered as a main optical transparent window for tissues, as water has very small light absorption in this range. The 1000–1350 nm wavelength range is considered another window for in vivo imaging owing to relatively small light absorption, very small light scattering, and low (one-photon absorption induced) auto-fluorescence, and consequently the penetration of multiphoton excitation light can be efficiently improved.[13] Femtosecond (fs) pulsed laser is a promising light source for multiphoton excitation. With low average power, high peak power, and relatively low repetition period, a fs laser can be properly operated to

[*] Dr. J. Qian,[+] D. Wang,[+] F. H. Cai, Z. F. Zhu, Prof. S. He
Centre for Optical and Electromagnetic Research, Zhejiang Provincial Key Laboratory for Sensing Technologies, State Key Laboratory of Modern Optical Instrumentation, Zhejiang University (China)
and
JORCEP (Joint Research Center of Photonics of the Royal Institute of Technology (Sweden), Lund University (Sweden), and Zhejiang University (ZJU)), Hangzhou, Zhejiang, 310058 (China)
E-mail: sailing@kth.se
L. Peng, Prof. S. He
ZJU-SCNU Joint Research Center of Photonics, South China Normal University (SCNU), Guangzhou, 510006 (China)
Dr. W. Xi
Department of Neurobiology, Key Laboratory of Medical Neurobiology of Ministry of Health of China, Zhejiang Province Key Laboratory of Neurobiology, School of Medicine, Zhejiang University, Hangzhou, Zhejiang (China)
Dr. H. He, Prof. M. L. Hu
Ultrafast Laser Laboratory, College of Precision Instrument and Optoelectronics Engineering, Key Laboratory of Opto-Electronics Information and Technical Science, Ministry of Education, Tianjin University, Tianjin 300072 (China)
[+] These authors contributed equally to this work.

[**] This work was partially supported by the Science and Technology Department of Zhejiang Province, the National Basic Research Program (973) of China (2011CB503700), the Special Financial Grant from the China Postdoctoral Science Foundation (No. 201104741), the National Natural Science Foundation of China (61275190, 61008052, 61178062, and 60990322), and the Fundamental Research Funds for the Central Universities. J.Q. is grateful to Dr. S. S. Liu for help with two-photon laser scanning confocal microscopy. We also express our deepest gratitude towards Prof. Z. P. Xu's group for their help in the cell proliferation assay.

Supporting information for this article is available on the WWW under http://dx.doi.org/10.1002/anie.201206107.

produce a mimimal thermal effect during its interaction with biosamples, which can effectively avoid certain thermal damage. Under imaging guiding, a fs laser can also achieve cellular/subcellular behavior manipulation, for example, cell fusion, gene transfection, and Ca^{2+} influx control.[14]

Herein, we observe two-photon and three-photon induced photoluminescence from GO nanoparticles under fs laser excitation. The two-photon and three-photon absorption coefficients of GO nanoparticles at various wavelengths were also measured. Conjugated with PEG molecules, GO nanoparticles exhibited high chemical stability, and could effectively label HeLa cells. Imaged with a two-photon scanning microscope, GO nanoparticles were observed to localize in the mitochondria, endoplasmic reticulum, Golgi and lysosome of HeLa cells. Furthermore, we demonstrated the applications of GO-PEG nanoparticles as contrast agents for in vivo two-photon luminescence imaging for the first time. We intravenously injected GO-PEG nanoparticles into mice body from the tail vein, and observed their flow, distributions and clearance in the blood vessels, by utilizing a deep-penetrating two-photon imaging technique. We also microinjected GO-PEG nanoparticles into the brain of gene transfected mice, and the in vivo two-photon luminescence imaging results showed that GO nanoparticles located at 300 μm depth in the brain could be clearly distinguished.

GO nanoparticles were synthesized from bulk graphite with a modified Hummer's method (Figure 1 a). According to TEM analysis (Figure 1 b), the as-synthesized GO nanoparticles have an average size of about 40 nm. An atom force microscope (AFM) image shows that the average thickness of the as-synthesized GO nanoparticles was about 1 nm (Figure 1 c),[15] which was close to that of single-layer GO nanoparticles. Extinction spectra of an aqueous dispersion of GO nanoparticles was measured by a UV/Vis scanning spectrophotometer. As shown in Figure 1 d, the extinction intensity at a short wavelength is more distinct than at a long wavelength, and a distinct absorption peak at 230 nm can be observed, which was mainly induced by the electronic conjugation within the GO structure.[16] One-photon luminescence performance of GO nanoparticles was then measured by a fluorescence spectrophotometer with an excitation wavelength of 405 nm. The photoluminescence spectrum is in the range of 450 to 700 nm, with the maximum located at 550 nm (Figure 1 d). The excitation spectrum of GO nanoparticles was measured with emission wavelength set at 550 nm (Supporting Information, Figure S2). We also noticed that the one-photon luminescence spectra of GO nanoparticles under various excitation wavelengths were almost the same (Supporting Information, Figure S3). The one-photon luminescence measurements illustrate that although Rayleigh scattering by GO nanoparticles is not negligible, linear absorption still contributes much to the whole extinction.

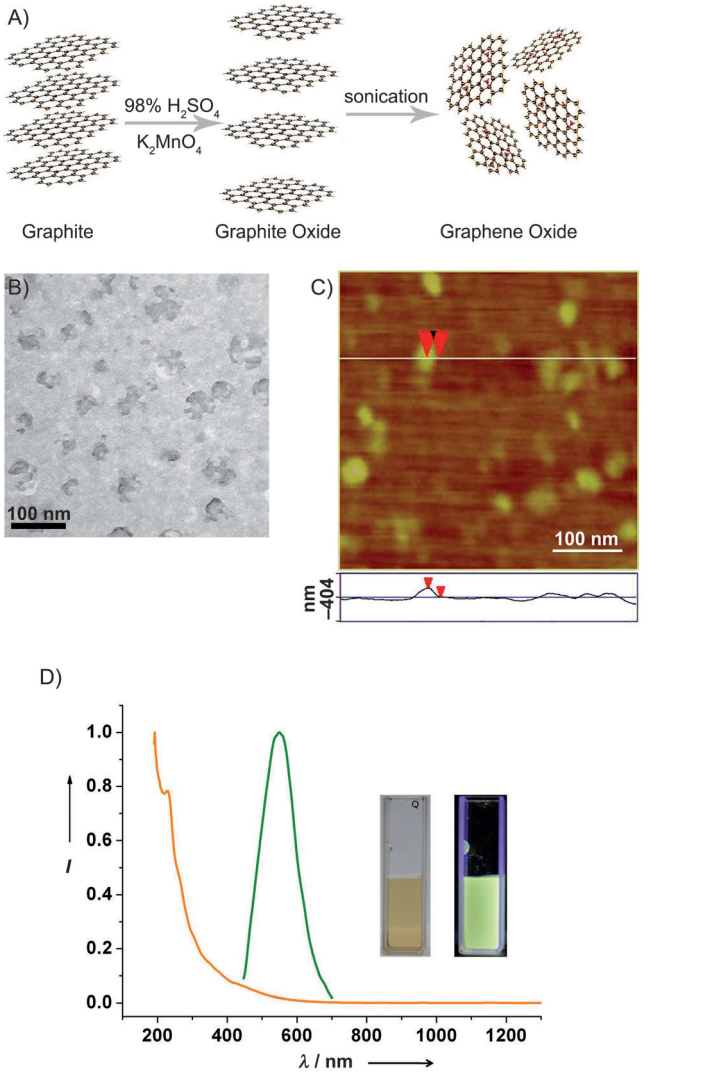

Figure 1. Synthesis and characterization of the GO nanoparticles. A) Synthesis of GO nanoparticles from bulk graphite; B) a TEM picture of GO nanoparticles; C) an AFM image of GO nanoparticles; D) extinction spectrum (orange line) and one-photon induced luminescence spectrum (green line) of an aqueous dispersion of GO nanoparticles (Inset: pictures of an aqueous dispersion of GO nanoparticles under daylight lamp irradiation (left) and UV lamp excitation (right)).

According to one-photon excitation and luminescence spectra of GO nanoparticles, a fs laser with a wavelength in the 700–900 nm range can be used for two-photon excitation. The linear transmission spectra of a 1 cm-thick layer of water and aqueous dispersion of GO nanoparticles was measured (Supporting Information, Figure S5), and both had negligible one-photon attenuation in the 700–900 nm range. We used an 810 nm, circa 150 fs (Ti-sapphire, Mira HP, Coherent, Inc.) pulsed laser at a repetition rate of 80 MHz for two-photon study of aqueous dispersion of GO nanoparticles in a cuvette (0.05 mg mL^{-1}). The luminescence spectrum was recorded with an optical fiber spectrometer (PG2000, Ideaoptics Instruments). As shown in Figure 2 a, the two-photon luminescence spectrum of GO nanoparticles is in the range of 400 to 700 nm (with the maximum located at 550 nm), and its

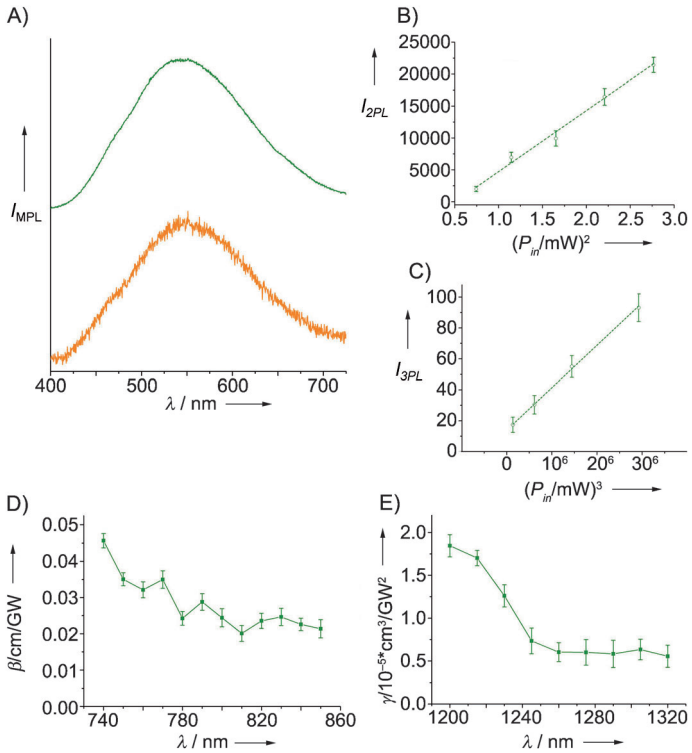

Figure 2. Multiphoton excited behaviors of GO nanoparticles. a) Two- (green; 810 nm 80 MHz laser) and three-photon induced (orange; 1260 nm, 80 MHz) luminescence spectra of GO nanoparticles; b) square dependence of two-photon induced luminescence P_{in}/W on the excitation intensity I_{2PL} of the 810 nm 80 MHz fs laser; c) cube dependence of three-photon induced luminescence on excitation intensity of of the 1260 nm, 80 MHz fs laser; d) two-photon absorption coefficient β of GO nanoparticles in water ($c = 0.2$ mg mL^{-1}; 150 fs, 80 MHz laser pulses); e) three-photon absorption coefficient γ of GO nanoparticles in DMSO ($c = 0.2$ mg mL^{-1}; 130 fs, 1 kHz laser pulses).

envelope is very similar to that under one-photon excitation (green line in Figure 1 d). Therefore, in both one-photon and two-photon processes, the excited GO nanoparticles were finally relaxed to the same lowest excited electronic–vibrational state(s) from which the luminescence emission occurred. Thus, when the GO sample is stimulated by 810 nm laser pulses, it needs to absorb at least two photons at the same time to be excited (Supporting Information, Figure S6a).[17] To verify that the observed luminescence was induced by two-photon excitation, we measured a series of emission intensities of GO nanoparticles under fs laser excitation (at 810 nm) with various average powers. The luminescence intensity dependence on the excitation intensity is plotted and shown in Figure 2 b, where one can see that the two-photon induced emission intensity is proportional to the square of the fs excitation intensity, confirming the characterization of a two-photon process. The preliminary two-photon induced quantum yield of GO nanoparticles (0.05 mg mL^{-1} in aqueous dispersion) was estimated to be about 5.809×10^{-4} % according to a relative measurement.[18] The two-photon induced luminescence feature of GO nanoparticle facilitates its wide applications in two-photon microscopy-based bioimaging, which can achieve higher spatial resolution (see the Supporting Information), deeper imaging range and less photobleaching. Furthermore, GO nanoparticles with two-photon absorption properties can also be utilized in other fields, such as power limiting, optical stabilization, and optical reshaping.[19]

We then used a 1260 nm, circa 100 fs pulsed laser at a repetition rate of 80 MHz to perform the measurement of three-photon induced luminescence of GO nanoparticles. The one-photon absorption of water at the 1260 nm wavelength is not so strong (Supporting Information, Figure S5). The fs laser source is based on a 1040 nm, 80 MHz, and 100 fs amplified output of a large-mode-area ytterbium-doped PCF oscillator. The output light was guided into a specifically designed all-solid photonic band-gap fiber to achieve 100 fs, 80 MHz, and continuously tunable wavelength ranging from 1160 to 1280 nm based on the soliton self-frequency shift principle. The maximum average power of this fiber fs laser can reach 400 mW, and the laser beam was introduced into an objective (40X, NA = 0.6) to achieve tight focus and high excitation intensity towards GO nanoparticles (0.05 mg mL^{-1}). The envelope of the three-photon induced luminescence spectrum is similar to those under one-photon and two-photon excitations. Similar to the principal of two-photon luminescence, when the GO sample is stimulated by 1260 nm laser pulses, it needs to absorb at least three-photons at the same time to be excited (Supporting Information, Figure S6b) and then relax to the same lowest excited electronic–vibrational state(s) to produce luminescence emission.[17] Various three-photon induced emission intensities of GO nanoparticles were then obtained under fs laser excitation with different average powers, and its intensity dependence on the pump pulse energy is shown in Figure 2 c. The three-photon induced emission intensity is proportional to the cube of the fs excitation intensity, which verifies the characterization of a three-photon process. Although three-photon luminescence behaviors of several materials (e.g., noble metal nanoparticles, quantum dots, and organic dyes) has been reported,[20] herein we observed for the first time three-photon induced luminescence performance from GO nanoparticles. In the wavelength range of 1000–1350 nm, the penetration depth of 1260 nm three-photon excitation light can be improved owing to low light scattering, and GO nanoparticles can be used as contrast agents for three-photon microscopy imaging. Because of longer wavelength excitation, three-photon microscopy may not be helpful to improve the spatial resolution of the imaging compared with (one-photon) confocal and two-photon microscopy (see the Supporting Information). However, owing to the higher-order dependence on excitation laser intensity, three-photon induced autofluorescence of cell and tissue can be greatly eliminated, which cannot be achieved in either (one-photon) confocal or two-photon microscopy.[20a] This advantage makes GO nanoparticle based three-photon microscopy a potential method for low background and high contrast bioimaging. Three-photon absorption property of GO nanoparticles can also be applied in power limiting, optical stabilization, and optical reshaping, and its effects can

be more distinct compared with two-photon excitation as it requires a higher excitation laser intensity to achieve a higher-order nonlinear effect.[19b] Furthermore, the three-photon absorption of GO can be excited by a pulsed laser with a wavelength of 1500–1600 nm,[19e] and thus the optical stabilization and optical reshaping effects are very helpful to various optical communication and signal processing applications. We believe that GO based three-photon absorption and luminescence features have great potentials in bioimaging, military protection and optical communication applications in the future.

We then present the results of our preliminary measurements of the two-photon absorption (2PA) coefficient as well as three-photon absorption (3PA) coefficient as a function of the excitation wavelength. The nonlinear transmissivity of a two-photon absorbing or a three-photon absorbing medium can be described by:[12b]

$$T(I_0,\lambda)=\frac{1}{1+\beta(\lambda)I_0L} \quad (1)$$

$$T(I_0,\lambda)=\frac{1}{\sqrt{1+2\gamma(\lambda)I_0^2L}} \quad (2)$$

where I_0 is the peak intensity of the incident light, L is the path length of the sample, $\beta(\lambda)$ is the 2PA coefficient (in units of $cm\,GW^{-1}$), and $\gamma(\lambda)$ is the 3PA coefficient (in units of $cm^3\,GW^{-2}$). Both these two coefficients depend on the excitation wavelength and the concentration of nonlinear absorbing centers (for example, the number of nanoparticles per cm^3) of the medium.

From the equation, it can be seen that, for a given excitation wavelength λ and input laser peak intensity value I_0, the corresponding nonlinear absorption coefficient $\beta(\lambda)$ or $\gamma(\lambda)$ can be calculated by measuring the nonlinear transmissivity value $T(I_0, \lambda)$ for a given sample medium. Thus, a complete 2PA or 3PA spectral curve can be obtained by discretely changing the excitation wavelength.

To measure the 2PA coefficient $\beta(\lambda)$ from 740 to 850 nm, in which the linear (one-photon) attenuation is very small, we performed nonlinear transmission measurements at twelve different excitation wavelengths with the Mira HP Ti-sapphire fs laser (80 MHz, tunable wavelength from 690 to 1040 nm). The laser beam was focused onto 1 cm long aqueous dispersion of GO nanoparticles ($0.2\,mg\,mL^{-1}$) in a cuvette. The measured data of 2PA coefficient as a function of the excitation wavelength are shown in Figure 2d, which shows a decrease of the β value from about $0.045\,cm\,GW^{-1}$ at 740 nm to around $0.023\,cm\,GW^{-1}$ in the 820–850 nm range.

To measure the 3PA coefficient $\gamma(\lambda)$ from 1200 to 1320 nm, we first transferred the dispersion of GO nanoparticles from water to DMSO, as water has very distinct linear attenuation in 1200–1320 nm (Supporting Information, Figure S5), while the one-photon absorption of DMSO in the wavelength range is very small.[21] We performed nonlinear transmission measurements at nine different excitation wavelengths with an optical parametric amplifier (OPA, 1 KHz, tunable wavelength from 239 nm to 20 μm, TOPAS, Coherent, Inc.) pumped by a Ti-sapphire oscillator and amplifier system (Mantis and Libra, Coherent, Inc.). The laser beam was focused onto a 1 cm long DMSO dispersion of GO nanoparticles ($0.2\,mg\,mL^{-1}$) in a cuvette. The measured data of the 3PA coefficient as a function of the excitation wavelength are shown in Figure 2e, which shows a decrease of the γ value from about $1.84\times10^{-5}\,cm^3\,GW^{-2}$ at 1200 nm to about $0.6\times10^{-5}\,cm^3\,GW^{-2}$ in the 1260–1320 nm range.

Prior to bioimaging applications, GO nanoparticles were grafted with PEG 2000 molecules following a modified previously reported procedure .[5b] By utilizing two-photon luminescence microscopy, we observed that GO-PEG nanoparticles can be uniformly taken up by HeLa cells (Supporting Information, Figures S12 and S13). We also investigated detailed distribution of GO-PEG nanoparticles in subcellular structures (for example, mitochondria, endoplasmic reticulum, Golgi, and lysosome) for the first time (Supporting Information, Figure S14). The investigation will be very helpful to illustrate some important cellular actions and to achieve functional cellular manipulation.

In recent years, GO has been utilized in various types of in vivo research, such as distribution monitoring, tumor targeting, photothermal therapy, and chemotherapeutic drug delivery.[5a,9c,22] However, no research group has ever extended their applications to animal blood-vessel and brain imaging. To achieve high imaging resolution and observe the detailed information, a confocal microscope rather than a macro in vivo imaging system should be adopted. In traditional one-photon confocal microscopy, visible excitation/emission light is prone to be absorbed by water in the tissue, and scattered owing to the Rayleigh scattering effect, so the imaging depth cannot reach 100 μm. As mentioned above, by virtue of less absorption/scattering of NIR fs excitation source, deep-tissue imaging capability is one of the advantages of two-photon luminescence microscopy. Furthermore, the nonlinear excitation mode can also help to improve spatial resolution of imaging rather than that under one-photon confocal microscopy. Considering the good performance of two-photon luminescence of GO nanoparticles, here we attempted to apply them in blood vessel imaging and brain imaging of live mice.

Figure 3 shows the in vivo two-photon blood vessel imaging results of mice at various time points after GO-PEG nanoparticle treatment. One hour after sample injection, bright two-photon luminescence was observed in the ear blood vessel of mice according to the overlay channel, while only autofluorescence could be obtained from the ear blood vessel of the control mice. As the two-photon signal was very distinct, intravenously injected GO-PEG nanoparticles can also reveal the vascular architecture as well as individual RBC (red blood cell), which appeared as shadows flowing with the two-photon fluorescent signals. A rapid line scan along the capillary axis, which is one of the functions of the commercial confocal microscope software, was then used to determine RBC flow parameters. RBCs moving through the capillary appeared as oblique shadows from which the instantaneous velocity (dx/dT) of each RBC can be determined accordingly (Supporting Information, Figure S15). Six hours post the treatment, the two-photon luminescence decreased in the blood vessel due to the clearance of GO-PEG over time with

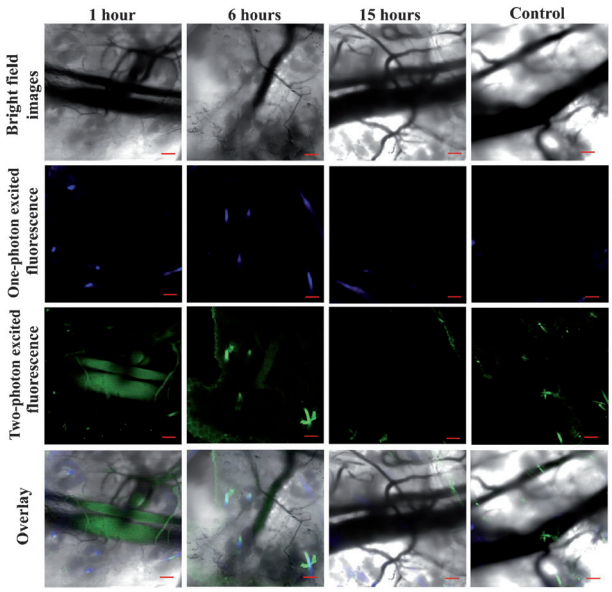

Figure 3. In vivo two-photon scanning and one-photon confocal luminescence imaging of intravenously injected GO nanoparticles in a blood vessel of a mice ear at various time points after sample treatment. Scale bar: 50 μm.

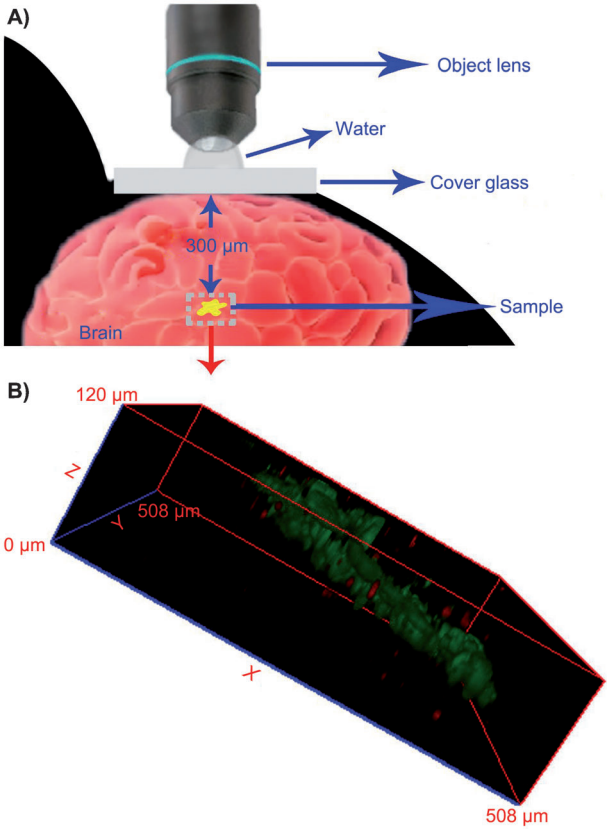

Figure 4. Two-photon luminescence imaging of GO nanoparticles in a mouse brain. a) Two-photon luminescence microscopy of a mouse brain; b) a reconstructed image of the three-dimensional distribution of GO-PEG nanoparticles.

a fast decay. 15 h after sample injection, almost no GO-PEG could be detected. For contrast, we also used a 405 nm-laser as excitation source to perform one-photon confocal imaging along with two-photon imaging. No luminescence signal could be detected from the blood vessel even when two-photon luminescence was most distinct one hour post GO-PEG treatment. It was mainly attributed to the absorption/scattering loss of 405 nm excitation in skin/blood, which greatly limited the imaging depth of in vivo one-photon confocal microscopy. It also confirmed that two-photon microscopy is a better solution for deep-tissue imaging.

Figure 4 shows two-photon luminescence microscopy of a mouse brain and corresponding a three-dimensional (3D) reconstructed image of GO-PEG nanoparticles in the mouse brain. A 3D reconstructed picture with free 360° rotation is shown in the Supporting Information. For two-photon excitation of GO nanoparticles, 810 nm fs laser was adopted, and a filter ranging from 500 nm to 575 nm was used to extract the two-photon induced emission signals from GO. As the oligodendrocyte progenitor cells in the mouse brain was stained with DsRed through gene transfection, 980 nm fs excitation was adopted and a wavelength filter ranging from 600 nm to 675 nm was used to extract the fluorescence signals of DsRed. The two-photon luminescence of GO nanoparticles (green), as well as that of DsRed (red), could be observed under the background and be easily discriminated from each other. It clearly illustrated that the microinjected GO-PEG nanoparticles distributed in a 500 μm 500 μm 120 μm space at a depth of about 300 μm in the mouse brain. Owing to the diffusion of microinjected GO-PEG in the brain, which cannot be eliminated in practical experiments, the green emitted GO-PEG nanoparticles took on some bright stripes. The red fluorescence indicated the DsRed dye stained the oligodendrocyte progenitor cells very uniformly through gene transfection. Usually, the distribution depth of cerebellum, cerebral cortex, and cerebral cortex blood vessels of small mice were not beyond 800 μm in their brains. If the photoluminescence of GO is tuned to a deep red/NIR region and the fs laser excitation condition can be further optimized, GO-based two-photon excitation can achieve such an imaging depth, and it will be very helpful to various potential in vivo applications (such as gene therapy in the brain or blood–brain barrier penetration).[23] Furthermore, the fs laser can also assist in the manipulatation of cellular/tissue behaviors additional to multiphoton excitation.

In summary, two-photon and three-photon induced luminescence of GO nanoparticles were clearly observed by utilizing fs pulse laser excitation. We also measured the two-photon and three-photon absorption coefficients of GO nanoparticles. Grafted with PEG molecules, GO nanoparticles exhibited high chemical stability under various pH values. GO-PEG nanoparticles were also shown to have negligible cytotoxicity by a cell proliferation assay and histological analysis, which could facilitate their in vitro and in vivo applications. In in vitro cell imaging, two-photon luminescence imaging clearly illustrated the distribution of GO-PEG nanoparticles in cellular/subcellular components. In in vivo imaging, we intravenously injected GO-PEG nanoparticles into mice body from the tail vein, and observed their flow, distributions, and clearance in blood vessels by utilizing

a deep-penetrating two-photon imaging technique. We also microinjected GO-PEG nanoparticles into the mice brain. The nanoparticles could easily be discriminated with two-photon luminescence microscopy, and the imaging depth could reach 300 μm or more.[24]

Received: July 30, 2012
Published online: September 24, 2012

Keywords: bioimaging · graphene oxide · multiphoton induced luminescence · subcellular imaging

[1] K. S. Novoselov, A. K. Geim, S. V. Morozov, D. Jiang, Y. Zhang, S. V. Dubonos, I. V. Grigorieva, A. A. Firsov, *Science* **2004**, *306*, 666.

[2] a) K. S. Novoselov, A. K. Geim, S. V. Morozov, D. Jiang, M. I. Katsnelson, I. V. Grigorieva, S. V. Dubonos, A. A. Firsov, *Nature* **2005**, *438*, 197; b) C. Lee, X. D. Wei, J. W. Kysar, J. Hone, *Science* **2008**, *321*, 385.

[3] a) Z. Sun, T. Hasan, F. Torrisi, D. Popa, G. Privitera, F. Wang, F. Bonaccorso, D. M. Basko, A. C. Ferrari, *ACS Nano* **2010**, *4*, 803; b) X. Ling, L. Xie, Y. Fang, H. Xu, H. Zhang, J. Kong, M. S. Dresselhaus, J. Zhang, Z. Liu, *Nano Lett.* **2010**, *10*, 553; c) X. Li, Y. Zhu, W. Cai, M. Borysiak, B. Han, D. Chen, R. D. Piner, L. Colombo, R. S. Ruoff, *Nano Lett.* **2009**, *9*, 4359.

[4] a) K. P. Loh, Q. Bao, G. Eda, M. Chhowalla, *Nat. Chem.* **2010**, *2*, 1015; b) L. Feng, Z. Liu, *Nanomedicine* **2011**, *6*, 317.

[5] a) X. Zhang, J. Yin, C. Peng, W. Hu, Z. Zhu, W. Li, C. Fan, Q. Huang, *Carbon* **2011**, *49*, 986; b) C. Peng, W. Hu, Y. Zhou, C. Fan, Q. Huang, *Small* **2010**, *6*, 1686.

[6] a) J. Qian, K. Yong, I. Roy, T. Y. Ohulchanskyy, E. J. Bergey, H. H. Lee, K. Tramposch, S. He, A. Maitra, P. N. Prasad, *J. Phys. Chem. B* **2007**, *111*, 6969; b) J. Qian, L. Jiang, F. Cai, D. Wang, S. He, *Biomaterials* **2011**, *32*, 1601; c) Q. Zhan, J. Qian, H. Liang, G. Somesfalean, D. Wang, S. He, Z. Zhang, S. Andersson-Engels, *ACS Nano* **2011**, *5*, 3744.

[7] S. Shukla, S. Saxena, *Appl. Phys. Lett.* **2011**, *98*, 073104.

[8] W. Zhang, Z. Guo, D. Huang, Z. Liu, X. Guo, H. Zhong, *Biomaterials* **2011**, *32*, 8555.

[9] a) X. Sun, Z. Liu, K. Welsher, J. T. Robinson, A. Goodwin, S. Zaric, H. Dai, *Nano Res.* **2008**, *1*, 203; b) Z. Liu, J. T. Robinson, X. Sun, H. Dai, *J. Am. Chem. Soc.* **2008**, *130*, 10876; c) K. Yang, S. Zhang, G. Zhang, X. Sun, S. T. Lee, Z. Liu, *Nano Lett.* **2010**, *10*, 3318.

[10] a) G. Eda, Y. Y. Lin, C. Mattevi, H. Yamaguchi, H. A. Chen, I. S. Chen, C. W. Chen, M. Chhowalla, *Adv. Mater.* **2010**, *22*, 505; b) J. Chen, X. Yan, *Chem. Commun.* **2011**, *47*, 3135; c) Z. Liu, X. Zhao, X. Zhang, X. Yan, Y. Wu, Y. Chen, J. Tian, *J. Phys. Chem. Lett.* **2011**, *2*, 1972; d) Z. Liu, Y. Wang, X. Zhang, Y. Xu, Y. Chen, J. Tian, *Appl. Phys. Lett.* **2009**, *94*, 021902.

[11] a) S. Kim, H. E. Pudavar, A. Bonoiu, P. N. Prasad, *Adv. Mater.* **2007**, *19*, 3791; b) H. Wang, T. B. Huff, D. A. Zweifel, W. He, P. S. Low, A. Wei, J. X. Cheng, *Proc. Natl. Acad. Sci. USA* **2005**, *102*, 15752; c) K. T. Yong, J. Qian, I. Roy, H. H. Lee, E. J. Bergey, K. M. Tramposch, S. He, M. T. Swihart, A. Maitra, P. N. Prasad, *Nano Lett.* **2007**, *7*, 761.

[12] a) G. S. He, Q. Zheng, K. T. Yong, A. I. Ryasnyanskiy, P. N. Prasad, A. Urbas, *Appl. Phys. Lett.* **2007**, *90*, 181108; b) G. S. He, Q. Zheng, K. T. Yong, F. Erogbogbo, M. T. Swihart, P. N. Prasad, *Nano Lett.* **2008**, *8*, 2688.

[13] a) K. Welsher, S. P. Sherlock, H. J. Dai, *Proc. Natl. Acad. Sci. USA* **2011**, *108*, 8943; b) A. M. Smith, M. C. Mancini, S. Nie, *Nat. Nanotechnol.* **2009**, *4*, 710.

[14] a) H. He, K. T. Chan, S. K. Kong, R. K. Y. Lee, *Appl. Phys. Lett.* **2009**, *95*, 233702; b) H. He, K. T. Chan, S. K. Kong, R. K. Y. Lee, *Appl. Phys. Lett.* **2008**, *93*, 163901; c) H. He, S. K. Kong, R. K. Y. Lee, Y. K. Suen, K. T. Chan, *Opt. Lett.* **2008**, *33*, 2961; d) H. He, S. K. Kong, K. T. Chan, *J. Biomed. Opt.* **2010**, *15*, 059803.

[15] D. Li, M. B. Müller, S. Gilje, R. B. Kaner, G. G. Wallace, *Nat. Nanotechnol.* **2008**, *3*, 101.

[16] J. T. Robinson, S. M. Tabakman, Y. Y. Liang, H. L. Wang, H. S. Casalongue, D. Vinh, H. J. Dai, *J. Am. Chem. Soc.* **2011**, *133*, 6825.

[17] G. S. He, L. S. Tan, Q. Zheng, P. N. Prasad, *Chem. Rev.* **2008**, *108*, 1245.

[18] S. Fery-Forgues, D. Lavabre, *J. Chem. Educ.* **1999**, *76*, 1260.

[19] a) Q. D. Zheng, S. K. Gupta, G. S. He, L. S. Tan, P. N. Prasad, *Adv. Funct. Mater.* **2008**, *18*, 2770; b) G. S. He, Q. D. Zheng, C. G. Lu, P. N. Prasad, *IEEE. J. Quantum. Electron.* **2005**, *41*, 1037; c) G. S. He, L. X. Yuan, J. D. Bhawalka, P. N. Prasad, *Appl. Opt.* **1997**, *36*, 3387; d) G. S. He, J. Swiatkiewicz, Y. Jiang, P. N. Prasad, B. A. Reinhardt, L. S. Tan, R. Kannan, *J. Phys. Chem. A* **2000**, *104*, 4805; e) G. S. He, K. T. Yong, J. Zhu, H. Y. Qin, P. N. Prasad, *IEEE. J. Quantum. Electron.* **2010**, *46*, 931.

[20] a) L. Tong, C. M. Cobley, J. Chen, Y. Xia, J. X. Cheng, *Angew. Chem.* **2010**, *122*, 3563; *Angew. Chem. Int. Ed.* **2010**, *49*, 3485; b) C. Lu, W. Huang, J. Luan, Z. Lu, Y. Qian, B. Yun, G. Hu, Z. Wang, Y. Cui, *Opt. Commun.* **2008**, *281*, 4038; c) G. S. He, K. T. Yong, Q. Zheng, Y. Sahoo, A. Baev, A. I. Ryasnyanskiy, P. N. Prasad, *Opt. Express* **2007**, *15*, 12818.

[21] G. S. He, T. C. Lin, S. J. Chung, Q. D. Zheng, C. G. Lu, Y. P. Cui, P. N. Prasad, *J. Opt. Soc. Am. B* **2005**, *22*, 2219.

[22] L. Zhang, J. Xia, Q. Zhao, L. Liu, Z. Zhang, *Small* **2010**, *6*, 537.

[23] a) A. C. Bonoiu, S. D. Mahajan, H. Ding, I. Roy, K. T. Yong, R. Kumar, R. Hu, E. J. Bergey, S. A. Schwartz, P. N. Prasad, *Proc. Natl. Acad. Sci. USA* **2009**, *106*, 5546; b) D. J. Bharali, I. Klejbor, E. K. Stachowiak, P. Dutta, I. Roy, N. Kaur, E. J. Bergey, P. N. Prasad, M. K. Stachowiak, *Proc. Natl. Acad. Sci. USA* **2005**, *102*, 11539.

[24] Just before the first submission of our previous version of this manuscript (see http://arxiv.org/abs/1202.1975), we noticed a related work, which is on two-photon- (but not three-photon)-induced fluorescence and two-photon bioimaging (but not in vivo), has been published in this journal: J. L. Li, H. C. Bao, X. L. Hou, L. Sun, X. G. Wang, M. Gu, *Angew. Chem.* **2012**, *124*, 1866; *Angew. Chem. Int. Ed.* **2012**, *51*, 1830.

